JMEPEG (2008) 17:330–339
DOI: 10.1007/s11665-008-9207-7

1059-9495/$19.00

The Effect of Adhesion and Tensile Properties on the Formability of Laminated Steels

Robert B. Ruokolainen and David R. Sigler

(Submitted October 29, 2007; in revised form February 4, 2008)

Laminated steel has been implemented in vehicle structures by several automotive manufacturers to reduce in-cabin noise. This study provides an understanding of how the adhesion between the steel skin and the viscoelastic polymer core affects laminate formability. Material properties, including peel strength, shear strength, and tensile strength were determined. The presence of the viscoelastic core was found to slightly reduce tensile properties of the laminate compared to the skin sheet. Forming limit diagrams were also determined. These indicated that the viscoelastic core properties can significantly affect formability of laminated steel compared to that of solid steel sheet. In general, the formability of laminated steel was found to be similar to or less than that of the much thinner skin sheet material, which indicates that its formability should be less than that of solid steel of the same gauge.

Keywords automotive, carbon/alloy steels, mechanical testing, stamping

1. Introduction

In-cabin sound quality is a key characteristic of vehicle performance. Noise and vibration within the passenger compartment can be reduced by several different methods. Among the more effective methods is constrained layer damping, such as that employed by laminated steels.

Laminated steel is a ''sandwich''-type composite consisting of two outer metal sheets (skin sheets) bonded to a viscoelastic core. This type of laminated steel construction utilizes the constrained layer damping method to achieve good acoustic performance. The damping mechanism is such that under cyclic loading, the viscoelastic cores are subjected to shear strains; the shearing allows the transfer of vibration energy into heat energy which is dissipated into the materials. It is a more effective way to reduce panel vibration compared to extensional damping that occurs when the damping material is applied to only one side of the sheet metal panel.

The construction of this material, that is, thin metal skins with core thicknesses between 25 and 40 μm (Ref 1), can affect manufacturability. Thus, it is necessary to understand the behavior of laminated steels in order to develop appropriate manufacturing methods that will ensure long-term durability. Tensile and adhesive properties, including T-peel strength and tensile shear strength, and formability of three laminated steels each constructed with a different viscoelastic core were evaluated in this research.

Forming of laminated steel can lead to several issues during manufacturing. During stamping, areas that experience high strain levels can produce necks and splits through either one or both of the steel sheet layers. When such splitting occurs, it can be attributed, in part, to the thinner gauge of each layer of steel compared to a solid sheet for the same application. However, the viscoelastic core can play an important role. The core stiffness, adhesive strength and interfacial interaction define a system of coupled behaviors that will influence the sheets to either act independently, i.e., weakly coupled, or as strongly coupled such that formability can vary greatly. If the viscoelastic core is weak, it may act as a lubricant between the layers to allow the sheets to slide relative to one another, in which case the laminate acts as two independent thinner sheets rather than a single thick sheet, which may encourage premature splitting. On the other hand, if the core provides too strong of an adhesion between the sheets, it may adversely affect formability.

Aside from the propensity to split, experience has shown that laminated steel panels have a greater tendency to wrinkle during forming than a single sheet. This is considered to be caused, in part, by the viscoelastic core not securely bonded to the sheets in areas of the panel that experience draw-in. In this case, the two sheets can act independently and might be more prone to wrinkling than a single thicker sheet.

Another undesirable behavior that can be observed during forming is delamination around flanged areas. During the flanging process, the laminated steel is bent around a tight radius. The inner sheet in contact with the die is bent with a tighter radius than the outer sheet. The difference in length of line around the die for the two sheets can cause significant shear forces in the viscoelastic core. A weakened core may result in delamination under these conditions. In addition, retraction of the flanging tool can lift the outer layer of the laminate away from the inner layer applying very high stresses on the viscoelastic core, which can further contribute to delamination.

This article was presented at Materials Science & Technology 2007, Automotive and Ground Vehicles symposium held September 16-20, 2007, in Detroit, MI.

Robert B. Ruokolainen and **David R. Sigler**, General Motors R&D, 30500 Mound Rd., 480-106-212, Warren, MI 48090-9055. Contact e-mail: robert.b.ruokolainen@gm.com.

Welding is another operation that is sensitive to the properties of the viscoelastic core material. During spot welding, the viscoelastic core is heated and put under pressure by the welding electrodes. In order to improve welding performance, the viscoelastic core should be able to flow away from the weld location under heat and pressure to allow formation of a weld. Thus, its flow characteristics under heat and pressure are important. In addition, heat produced by the resistance spot weld can decompose the core material locally, producing both high gas pressure and a delaminated area around the weld (Ref 2, 3). The size and stability of the delaminated area are affected by the properties of the polymer core.

The above discussion illustrates the importance of the viscoelastic core properties as related to manufacturing processes. This work was intended to understand the relationship between the mechanical properties of both the viscoelastic core and laminate material and the resultant formability in automotive manufacturing of three types of viscoelastic core constructions. The results will provide a baseline of knowledge for laminated steel performance.

2. Experimental

2.1 Materials

Three different types or types of laminated steel samples, referred to as types A, B, and C, were differentiated by their viscoelastic cores. Where type A is an olefinic rubber-based polymer, type B is an acrylic-based polymer and C is an epoxy-based polymer. Also, laminated steels from type B included samples that represented bad formability (rejected material) as noted by a GM stamping facility. Gauges of the laminated steel were either 0.9 or 1.1 mm.

The mass per unit area of the viscoelastic core was determined for each material. Ten 50.8 mm × 50.8 mm coupons were cut, weighed, and peeled apart. The core materials were then removed using acetone or toluene solvent. The two steel skins were weighed again and the difference between the initial and the final weight provided the mass of the core materials. Table 1 gives the thickness and other information of these laminated steel samples.

2.2 Sample Preparation

Both T-peel and lap-shear test samples were sheared from large laminated steel sheets along longitudinal and transverse rolling directions. The longitudinal edges of each sample were dry milled to remove damage from shearing. Final dimensions of the T-peel samples were 304.8 mm × 25.4 mm with the first 76.2 mm peeled apart to allow for grip placement. The lap-shear samples were machined with one slot on either side of the metal skin, the final sample dimensions were 177.8 mm × 25.4 mm with an overlap width of 25.4 mm, as shown in Fig. 1. For each material 10-14 samples were prepared and tested at ambient temperature and humidity.

Table 1 Technical data of laminated steel samples

Sample type	Nominal overall thickness, mm	Core mass/unit area, g/m^2	Adhesive thickness, mm	Viscoelastic core material base polymer
A0.9	0.90	38.75	0.031	Styrene
A1.1	1.10	34.10	0.035	Styrene
B0.9	0.90	38.75	0.035	Acrylic
B1.1	1.10	41.85	0.039	Acrylic
C1.1	1.10	49.60	0.042	Epoxy

2.3 180° T-Peel Test

The peel strength between the viscoelastic core and the steel skin was determined by a standard T-Peel test, as described in ASTM D 1876-01. The tests were conducted on a screw driven test machine at a crosshead rate of 254 mm/min. The T-peel strength is defined as the average load in N/mm of the specimen width required to separate the adherends, which is determined from the load-extension curve for the first 127 mm of peeling distance after the initial peak in load.

2.4 Lap-Shear Test

The tensile lap-shear strength between the steel skin and the viscoelastic core was measured by a standard lap-shear test, following ASTM D 1002-01, with the modification of the crosshead speed. Instead of the standard 1.3 mm/min, a crosshead speed of 5.0 mm/min was chosen for these tests, which were also conducted on a screw driven test machine.

2.5 Forming Limit Diagrams and Tensile Tests

Five sets of steel sheets were used for forming limit diagram (FLD) determination and tensile testing. FLD tests were conducted utilizing a Tinius Olsen BUP Ductometer. ASTM standard E2218-02 procedure was followed. Tensile tests were conducted on a servohydraulic load frame following ASTM standard E 8-04, E 517-00, and E 646-00.

Tensile properties were evaluated in the rolling direction (rd), and at 45° and 90° to the rolling direction. FLDs along with tensile data were generated for laminated steel from all

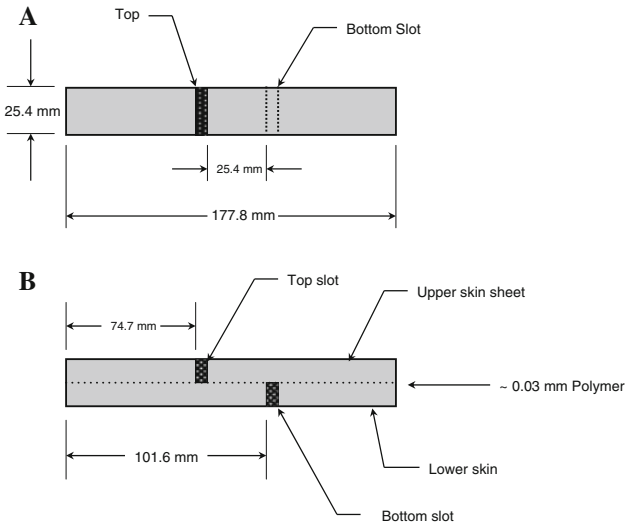

Fig. 1 Lap-shear specimen created by machining one slot in each layer of the laminated steel sheet. (a) Plan view: slot width of 1.5 mm and (b) Side view: slot depth of ~0.5 mm

three types, all 1.1-mm thick. FLDs and tensile data for skin sheets of the 1.1-mm thick laminate from types A and B material were also generated. Type C skin sheet was unavailable for testing.

2.6 Analysis Techniques

2.6.1 X-ray Photoelectron Spectroscopy (XPS). Immediately after conducting adhesive mechanical tests, samples were examined using XPS. Elemental survey scans were acquired on each skin sheet of the tested sample.

2.6.2 Scanning Electron Microscopy (SEM). Small sections were cut from both strips of various bulk samples after T-Peel tests and examined using a scanning electron microscope in a conventional secondary electron imaging mode. Accelerating voltages used were 15 and 20 kV. A thin film of Au was sputtered on the failure surfaces in order to reduce any charge build-up and increase the conductivity.

3. Results and Discussion

3.1 Adhesion Properties of Laminated Steels

3.1.1 180° T-Peel Strength. The results of T-peel strength tests for different laminated steels are listed in Table 2 and shown in Fig. 2. In general, for a given thickness the longitudinal and transverse values had a relative difference of less than 9%, with the type B laminate material exhibiting the largest relative difference of 16.1%. There was no preference for either the longitudinal or transverse samples to show higher T-peel strengths.

Table 2 Results of T-peel strengths of various laminated steels

Sample type	T-peel strength (longitudinal), N/mm	T-peel strength (transverse), N/mm
A0.9	1.690 ± 0.123	1.551 ± 0.029
A1.1	2.264 ± 0.091	2.434 ± 0.111
B0.9	2.271 ± 0.063	2.204 ± 0.069
B1.1	1.666 ± 0.070	1.958 ± 0.100
B1.1 (rejected)	1.811 ± 0.077	1.823 ± 0.062
C1.1	3.736 ± 0.224	4.022 ± 0.064

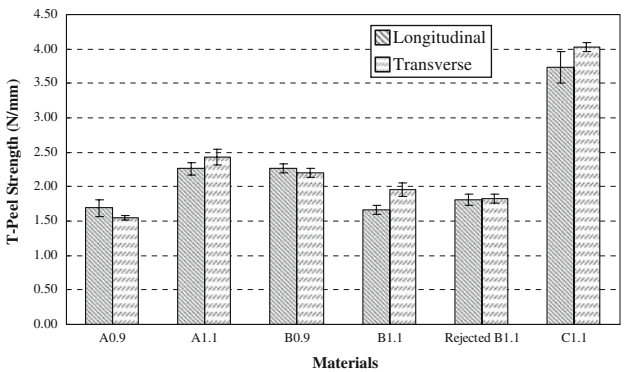

Fig. 2 T-peel strengths of laminated steels

Overall sheet thickness did not appear to influence T-peel strength in a consistent manner. The 1.1-mm thick A1.1 laminated steel had higher T-peel strengths than the 0.9-mm thick A0.9 material. The rejected B1.1 and original B1.1 laminate material had similar T-peel strengths, but these were 21% lower than the thinner B0.9 material.

The C1.1 laminated steel material was unusual in that it had significantly higher T-peel strengths than both A1.1 and B1.1. In the longitudinal direction, the T-peel strength of C1.1 was around 1.65 times that of A1.1, and around 2.24 times that of B1.1. In the transverse direction, the T-peel strength of C1.1 was around 1.65 times that of A1.1, and around 2.05 times that of B1.1.

3.1.2 Lap-Shear Strength. Results of the tensile lap-shear tests are listed in Table 3 and shown in Fig. 3. Similar to results for the T-peel tests, lap-shear test results for longitudinal and transverse samples of a given thickness had a relative difference of less than 12% except for the B0.9 material which had the largest difference of 22.0%.

Sheet thickness did not correlate strongly with shear strength. For type B laminate, the 1.1-mm thick material had shear strengths close to those for the 0.9-mm thick material. For type A material, however, the 1.1-mm thick material had much higher shear strengths than the 0.9-mm thick material. It is not clear why the shear strengths of the A1.1 material were nearly 3 times greater than those of the A0.9 material when compared to the T-peel strengths which indicate only a smaller increase for the A1.1 material by about 1.4 times. Thus, this difference may indicate variation in viscoelastic properties or how it is applied.

Table 3 Results of lap-shear strengths of various laminated steels

Sample type	Shear strength (longitudinal), MPa	Shear strength (transverse), MPa
A0.9	1.441 ± 0.248	1.281 ± 0.694
A1.1	3.973 ± 0.182	4.103 ± 0.069
B0.9	1.786 ± 0.121	1.432 ± 0.055
B1.1	1.653 ± 0.349	1.540 ± 0.085
B1.1 (rejected)	0.970 ± 0.114	1.042 ± 0.132
C1.1	5.084 ± 0.044	4.896 ± 0.053

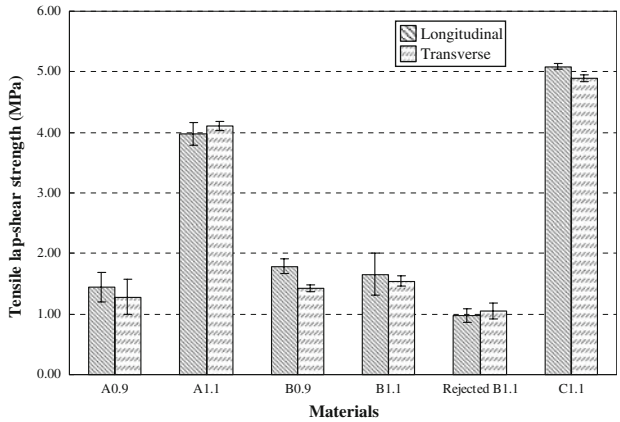

Fig. 3 Lap-shear strengths of laminated steels

Type C 1.1-mm thick laminate had higher shear strengths than both types A and B. In the longitudinal direction, the lap-shear strength of C1.1 was approximately 1.28 times that of A1.1, and approximately 3.08 times that of B1.1. In the transverse direction, the lap-shear strength of C1.1 was about 1.19 times that of A1.1, and approximately 3.18 times that of B1.1.

The results from both the T-peel and lap-shear tests for the types A and B materials provide a reference point for laminate adhesive properties. These two materials have been observed to delaminate during forming and welding. This suggests that increasing adhesive performance, that is, peel and shear strength, might help prevent delamination and improve both. The material from type C should provide an interesting comparison due to its superior adhesion behavior. Forming and corrosion tests performed with the C1.1 material may help determine the improvement in forming that can occur by increasing the adhesive properties.

3.2 Adhesive Failure Analysis

After the T-peel tests, XPS was used to examine the adhesive-adherent surfaces. These examined samples are shown in Fig. 4 with results listed in Table 4. The data suggest that for both A0.9 and A1.1 laminates adhesive failure occurred at either the steel/adhesive interface or the steel/contaminant interface based upon the detection of Fe on one of the skin sheets. The C1.1 laminate failure also appeared to be adhesive near the adhesive/galvanized interface as evidenced by the detection of Zn. For both B0.9 and B1.1 samples, the failure appeared to be cohesive, that is, within the adhesive, as neither Fe nor Zn was detected on the surface of the skin sheets.

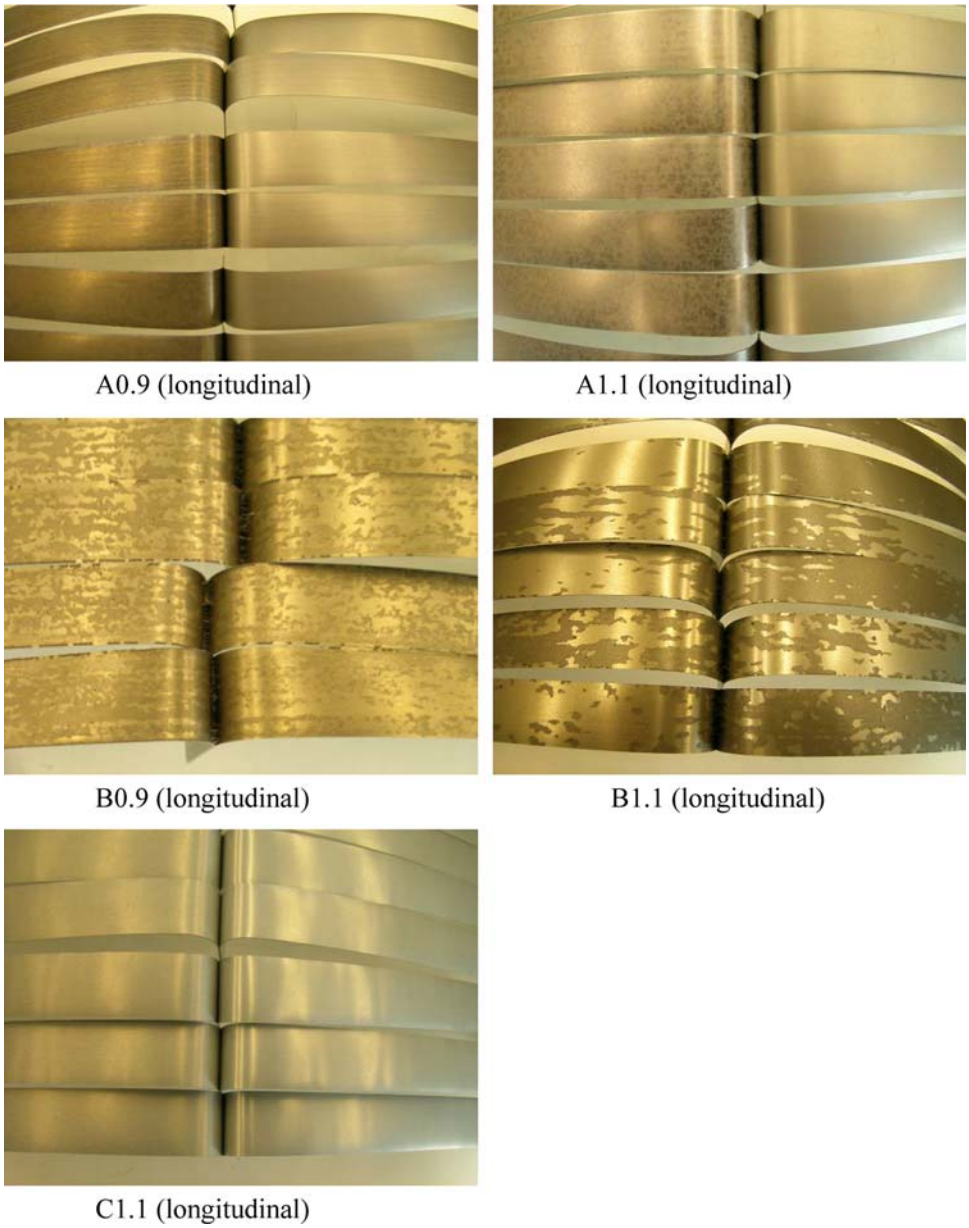

Fig. 4 Digital macrophotos of the fracture surfaces of laminated steels after T-peel tests

Table 4 Results of XPS semiquantitative elemental surface composition

Sample type		Atomic % (except H)										
		C	O	N	Fe	F	P	Ti	Mn	Zn	Si	Failure mode
A0.9	(Light side)	99	0.8	-	-	-	-	-	-	-	-	Adhesive
	(Dark side)	82	11	1.2	0.6	1.3	1.6	0.5	0.7	-	-	
A1.1	(Light side)	87	11	2.5	-	-	-	-	-	-	-	Adhesive
	(Dark side)	88	8	1.4	0.3	1.1	0.8	0.4	-	-	-	
B0.9	(Light side)	75	24	-	-	-	-	-	-	-	0.5	Cohesive
	(Dark side)	79	21	-	-	-	-	-	-	-		
B1.1	(Light side)	76	23	-	-	-	-	-	-	-	1.3	Cohesive
	(Dark side)	75	22	-	-	-	-	-	-	-	3	
C1.1	(Top Side)	80	19	-	-	-	-	-	-	-	0.8	Adhesive
	(Bottom Side)	73	23	-	-	-	-	-	-	0.7	2.8	

Combining macrophotographic evidence and the XPS analyses with the results of mechanical tests (strength values averaged over longitudinal and transverse directions for both 0.9-mm and 1.1-mm thicknesses), indicates that in these laminated steel samples, higher shear strength correlates with adhesive failure and lower shear strength correlates with cohesive failure. In T-peel test results, there was no correlation as the T-peel strengths for A (adhesive failure) and B (cohesive failure) materials were very nearly equal and both significantly lower than those of the C material (adhesive failure). Adhesive failure indicates that there is weak interaction between the surface of the substrate and the adhesive. Even at higher strengths, adhesive failure is considered to be an undesirable failure mode and cohesive failure is preferred. However, this criterion may not be valid for evaluating the adhesive strength of laminated steels.

SEM analysis was used to view the morphological features of polymer materials after testing. After T-peel testing, each sample was peeled apart to yield two metal strips, as shown in Fig. 4. SEM micrographs of separated T-peel samples are shown in Fig. 5. For both type A and type C laminated steel samples, the viscoelastic core materials adhered primarily to one skin sheet, which was defined as the adhesive-rich side, the other skin sheet with much less core material was defined as the adhesive-poor side. For type B samples, because core material was attached to both strips, no specific term was used to distinguish the two skin sheets. Observing the SEM micrographs of A0.9 material, the adhesive-rich side shows the metal surface was covered by the viscoelastic core with partially torn areas. However, on the adhesive-poor side, the metal surface was clearly visible with small areas sparsely decorated by torn pieces of the viscoelastic core. Even though chemical and thermal analyses of material A found that inorganic particles were components of the viscoelastic core, no evidence was observed from the SEM micrographs. This may be due to the small size of the conductive particles, which if wet by the viscoelastic core, would be effectively incorporated within it and, thus, hidden from view.

The SEM micrographs of C1.1 material, Fig. 5, show that the metal surface of the adhesive-rich side was covered by the viscoelastic core. However, compared with the A0.9 adhesive-rich side, a greater percentage of the viscoelastic core surface area was torn from the C1.1 adhesive-rich side. In addition, most of the tearing sites show a black hole surrounded by a gray annular ring. It appears as if solid particles were pulled out of the adhesive layer. On the adhesive-poor side of C1.1 material, the metal surface was clearly identified. The diameter of the single particles ranged between 6 and 15 μm. EDS analyses, Fig. 6, suggests that these were metal particles added to enhance conductivity within the viscoelastic core.

The SEM micrographs of adhesive failure surfaces of type B laminated steel show a large difference from those of types A and C. Both large and small regions of irregularly shaped particles were observed on both skin sheets. The size of these heterogeneous regions may reach as high as 400 μm. It appears that no significant polymer material was merged into these regions. These regions would provide no adhesion between the steel skin sheets. However, since the conductive particles appear to be present at a low volume percent, that is, ~1 vol.%, their effect on adhesive properties should be modest.

3.3 Tensile Tests and Forming Limit Diagrams

3.3.1 Tensile Tests. Tensile test data listed in Table 5 shows that all the tensile data were fairly consistent among the materials investigated with the skin sheet yield strengths being slightly higher than those of the corresponding laminated steel. Type C laminated steel had slightly better tensile properties than those of types A or B. It should be noted that the skin sheets of types A and B laminated steel both meet GM standards, thus their skin sheet tensile properties are expected to be very similar.

Figure 7-9 are examples of the true stress-true strain curves generated for laminated steels from types A, B, and C. In general the curves are similar among the samples tested, again with type C material having slightly higher values. Also, there appears to be no major differences for different orientations relative to the rolling direction.

On the basis of the tensile data, there appeared to be little difference between mechanical performance for laminates that might account for reported differences in formability during material tryout and production. In order to further investigate these reported differences in forming behavior, forming limit diagrams (FLD), were generated for these samples by physical testing.

3.3.2 Forming Limit Diagrams. Figure 10 shows the forming limit curves (FLCs) for types A, B, and C laminated steels of 1.1-mm thickness. The C1.1 laminated steel material exhibited similar formability as that of A1.1 on the left side of the FLD. In the biaxial strain region (right side of the FLD), the C1.1 material exhibited formability between that of the A1.1 and B1.1 materials. B1.1 laminated steel showed better

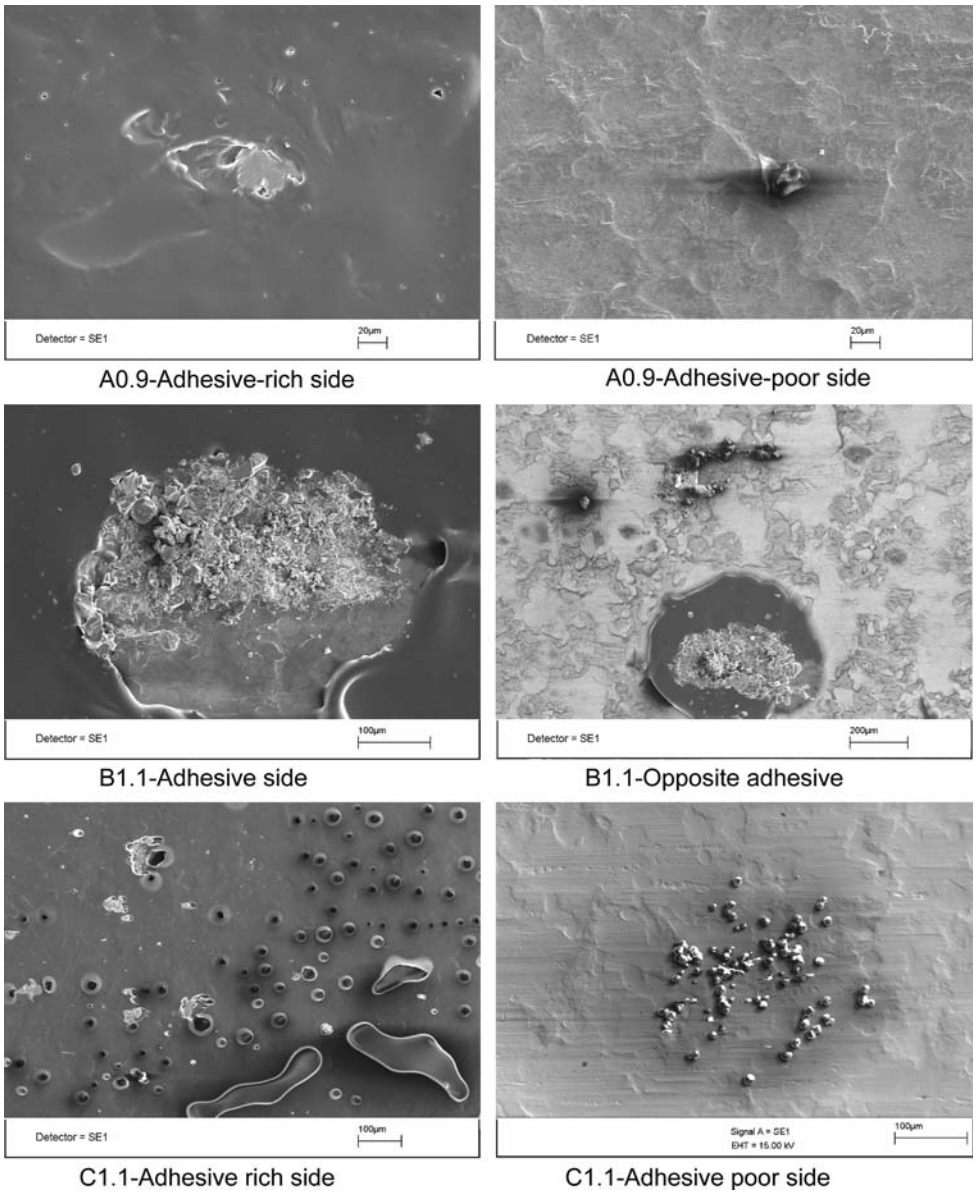

Fig. 5 SEM micrographs of the fracture surfaces of laminated steels after T-peel tests

formability in the biaxial region and slightly less formability on the left side of the FLD, although B1.1 material had better plane strain behavior (higher FLD_0) than the other two. A1.1 had the poorest plane strain behavior (FLD_0) of the three materials.

Figure 11 shows the FLCs for A1.1 and B1.1 skin sheet, that is, material without the polymer core. Type C skin sheet material was not available for testing. It should be noted that the marginal zone, that is, safety area defined by the forming limit curve and 10% below the forming limit curve, a feature that often accompanies FLDs, is not indicated in this work. The FLCs for A1.1 and B1.1 skin sheets were very similar; however, a noticeable difference in the forming limit curves for A1.1 and B1.1 laminates is evident in Fig. 10. For the plane strain condition into the biaxial strain region, laminate A1.1 formability was less than that of laminate B1.1. However, laminate A1.1 exhibited better formability on the left side of the FLD. Since the tensile properties and FLCs for A and B skin sheets were nearly identical, this difference in performance can most likely be attributed to differences in behavior of the viscoelastic core materials and the interface between the cores and skin sheets. In particular, both the A1.1 and C1.1 laminated steels had higher lap-shear strengths than did B1.1, as seen in Fig. 3. Figure 10 shows that A1.1 and C1.1 had similar forming behavior on the left side of the FLD.

Figure 12 further illustrates the effect of the viscoelastic cores by comparing the forming limit curves of A1.1 and B1.1 laminated steels to forming limit curves of their skin sheets. The addition of the viscoelastic core to the skin sheets significantly reduces type A laminated steel formability in the plane strain region and slightly reduces the formability of type B laminated steel in the draw-in region (left side of FLD) and the biaxial region (right side of the FLD).

It is well known that increasing steel sheet thickness in low strength steels provides significantly improved formability (Ref 4). Formability comparison of low carbon sheet steels of ~0.5 mm and ~1.0 mm show that the thicker material can

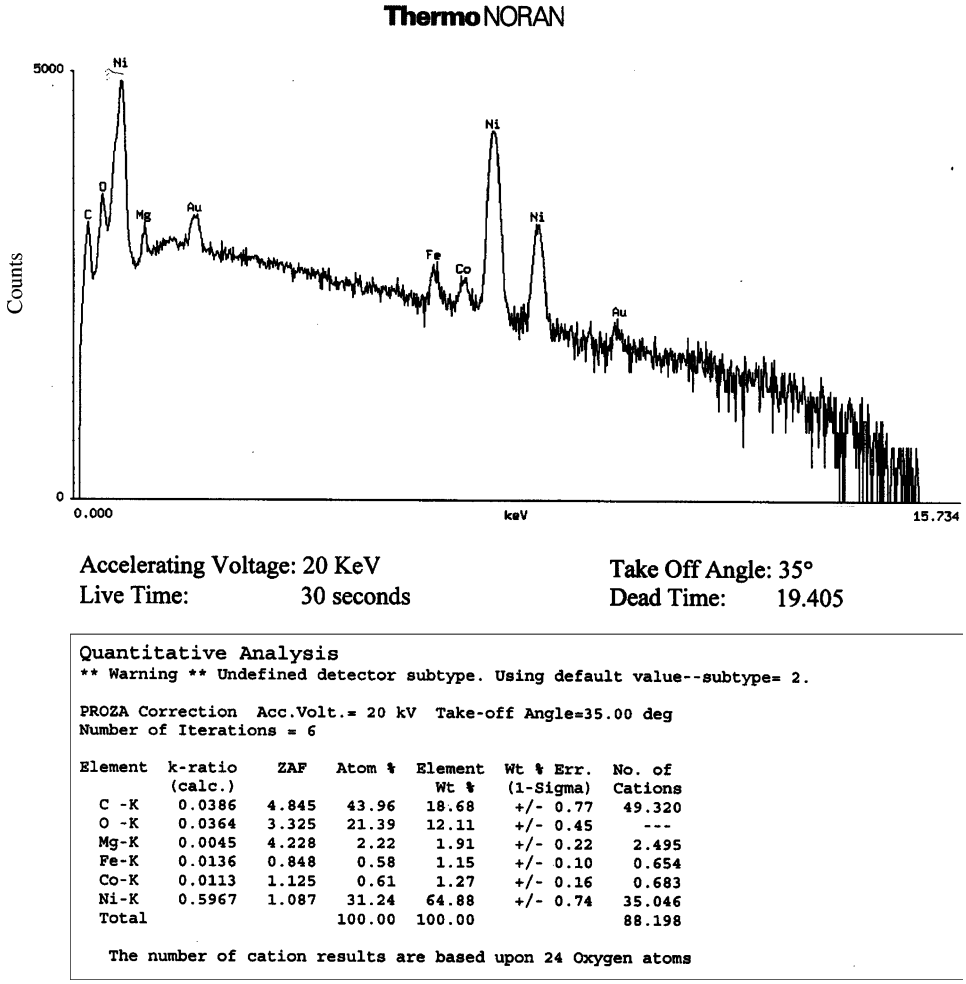

Fig. 6 SEM energy dispersive spectroscopy (EDS) results of the particle site on the C1.1 adhesive failure surface

Table 5 Laminated steel tensile data[a]

Specimen type	Angle from rolling direction, °	Yield strength, MPa	UTS, MPa	Elongation, %	*n*-Value	*r*-Value
A1.1	0	144	266	43.40	0.24	2.19
	45	148	264	47.05	0.24	2.31
	90	148	263	46.80	0.24	2.90
A1.1 skin sheet	0	153	277	44.25	0.24	1.98
	45	164	282	43.55	0.23	2.11
	90	161	275	43.35	0.24	2.79
B1.1	0	142	265	45.25	0.25	2.22
	45	144	258	47.70	0.24	2.41
	90	148	263	40.35	0.24	3.33
B1.1 skin sheet	0	158	286	42.95	0.24	2.17
	45	160	283	45.60	0.24	2.39
	90	160	280	44.60	0.24	3.11
C1.1[b]	0	152	293	47.35	0.26	1.97
	45	159	293	44.60	0.25	1.96
	90	156	289	44.00	0.25	2.51

[a]Values averaged over 2 samples
[b]Skin sheet samples were not available for these tests

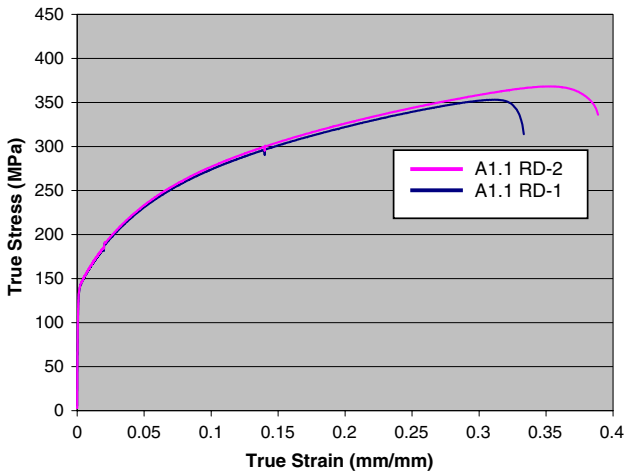

Fig. 7 True stress-true strain curve of A1.1 laminate in the rolling direction

attain ~7% greater forming strains than the thinner material across the entire field of minor strains (Ref 4). From Fig. 12, the formability of the laminated steel was at most equivalent to the skin sheets and could be somewhat worse. A similar observation was provided by Kim and Thompson (Ref 5), who compared bending force as a function of loading speed in four-point bend tests for laminated, monolithic and unbonded (skin sheet) sheets of the same total thickness (1.6 mm). The bending

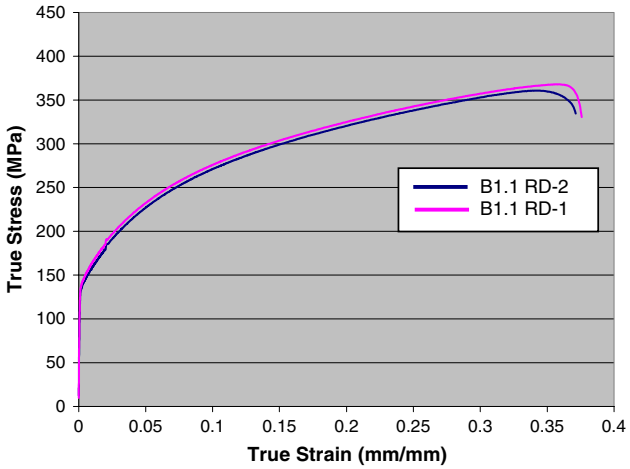

Fig. 8 True stress-true strain curve of B1.1 laminate in the rolling direction

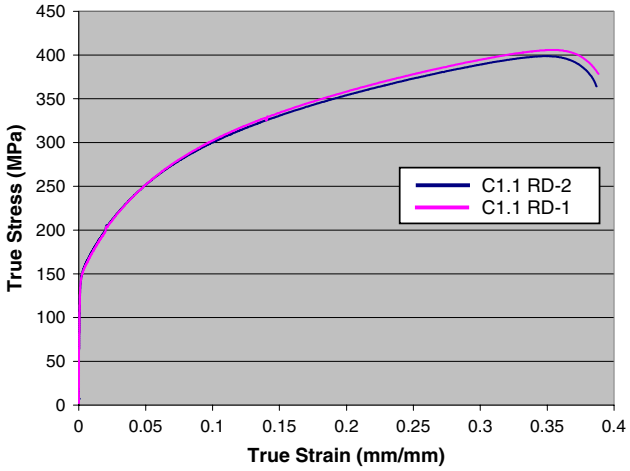

Fig. 9 True stress-true strain curve of C1.1 laminate in the rolling direction

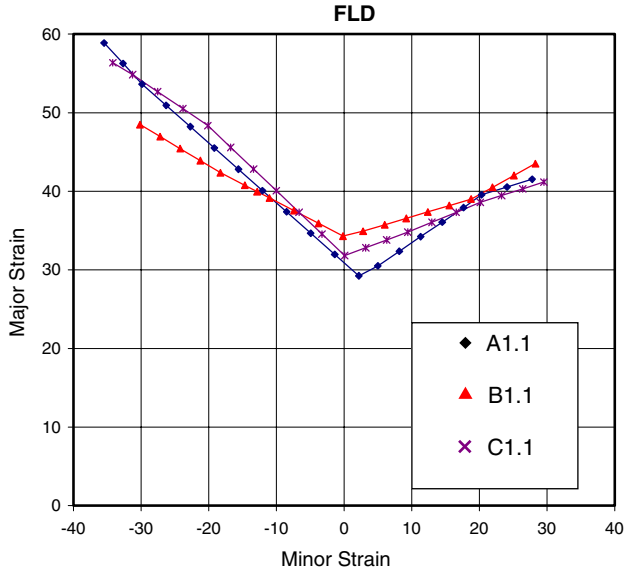

Fig. 10 Forming limit curves for A1.1, B1.1, and C1.1 laminated steels

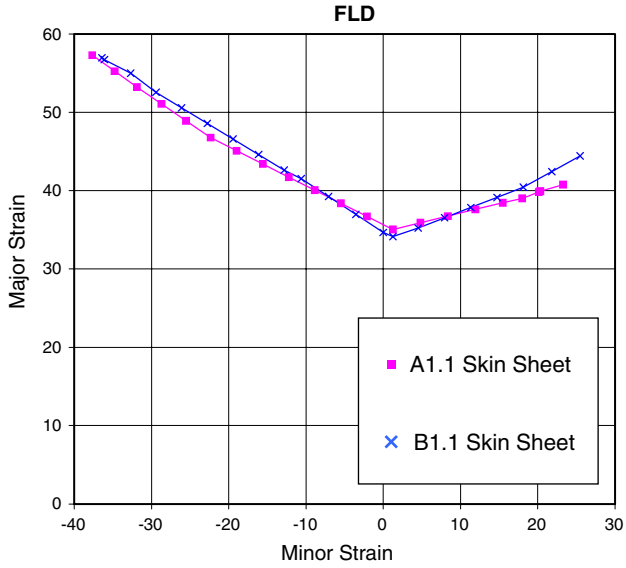

Fig. 11 Forming limit curves for A1.1 and B1.1 skin sheet

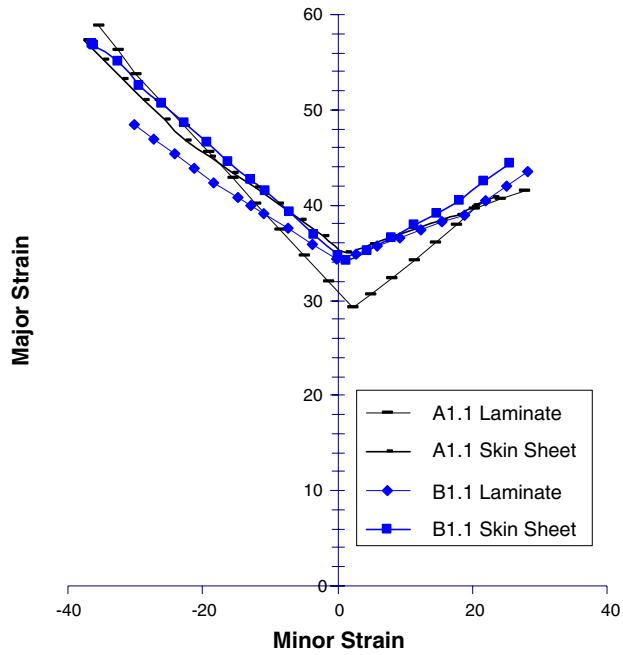

Fig. 12 Forming limit curve comparison of A and B 1.1-mm thick laminated steel versus their respective skin sheets

force of the laminated steel was slightly higher but much closer to the bending force of the skin sheet which had an interposed polytetrafluoroethylene sheet than the bending force of the monolithic steel sheet, which was approximately twice the skin sheet bending force. Thus, with these types of viscoelastic core materials the forming behavior of laminated steel more closely resembles the forming behavior of the skin sheets rather than monolithic steel of the same thickness.

The formability of laminated steel can be understood better by considering the criterion for determining the FLCs. The upper limit of formability is defined as the strain path that produces necking of one or both skin sheets. Each individual neck is confined to a localized area in the sheet. In order to

track the strain paths circle grids are first applied to the sheet material and samples of the material with various widths are bulge tested until failure occurs, that is, necking or cracking. For the balanced biaxial samples, a lock bead is used to completely secure the material around the circumference to prevent draw-in of material as the dome is driven into the sample. This produces samples with biaxially strained material near the poles with the highest positive minor strains. Narrow samples are completely secured at the ends and allow the width of the sample to move freely in order to examine the entire range of minor strain. For all samples, the deformed circle grid is then measured keeping track of those circles, which are near areas that have necking or cracks. The major and minor strains of circles/ellipses near the neck/crack are determined and plotted to give an upper limit to formability of the material.

Therefore, under these conditions it should not be possible for any laminate to have significantly better formability than a single skin sheet as shown in Fig. 12. Additionally, the laminate should have less formability than solid steel that is the same thickness as the laminate. As previously stated, Fig. 12 shows that in some minor strain regions laminate formability, in this case for laminate A1.1, is well below that of the thinner skin sheets, but in other regions the FLC of A1.1 approximates the skin sheet behavior. The following arguments may explain.

The left side of the FLD describes draw formability in which material is drawn in from the sides of the sample. One strain path on the left side is comparable to the uniaxial tensile test condition in which case the two skin sheets are pulled essentially in tension over the dome-shaped die with the viscoelastic core moving along with little influence. Figure 12 shows that in the draw region the laminates and skin sheets have similar formability, which agrees with the tensile test results.

For the balanced biaxial condition, the test sample was clamped fully around its perimeter. This should have the effect of locking the two sheets together around the periphery and limiting the relative motion and shear forces between the two sheets during forming, which should limit the influence of the viscoelastic core's mechanical behavior. That is, it is limited compared to other non-biaxial strain paths where there may be higher amounts of motion between skin sheets because there are varying constraints on the side edges as samples become narrower. Therefore, the laminate might behave very similarly to the skin sheet, as was observed for the balanced biaxial strains in Fig. 12.

In plane strain regions or regions of some positive minor strain, Fig. 12 indicates that the viscoelastic core can reduce formability compared to that of the skin sheets alone. In these regions, a material with a strong core such as the A1.1 laminate can transfer some shear load across the interface. Since the shear displacement is inversely proportional to the shear strength (Ref 6) this will put additional stress on the skin sheet. However, since the failure criterion is still localized necking or cracking in one of the skin sheets, formability is still strongly influenced by the individual skin sheet thickness. Thus, the traction from a stronger core could reduce formability as shown by the A1.1 material in Fig. 12.

However, if lap-shear strength of the viscoelastic core was the only criterion to affect formability, then the C1.1 laminate should have different formability than the A1.1 laminate due to laminate C1.1's higher shear strength (Fig. 3) and clearly this is not the case as illustrated in Fig. 10. Only in the negative minor strain region (>−10%) is there a direct, but weak correlation between lap-shear strength and formability for all three laminates. A possible explanation is that viscoelastic core materials may exhibit pressure-dependent flow behavior. The strain localization of the lower skin should be affected by hard contact and friction with the punch while the strain localization of the upper skin should be affected by the viscosity and shear strength of the viscoelastic core. The viscoelastic layer that has the ability to transmit compressive stresses more so than shear stresses (Ref 7) could be affected by pressure due to the compressive force of the punch and resistance to deformation of the upper skin.

To more fully understand the influence of the viscoelastic core on formability, additional research is required. Clearly, the forming dynamics of laminated steel is not simple and a given test may not capture the full complexity, thus, further research or different test methods are needed. Laminated steels with consistent skin sheet properties and a wide range of core properties are needed so that the influence of the core on final laminate forming properties is fully understood.

The reduced formability of A1.1 material in the plane strain and some of the biaxial region is not to suggest that this material has over-all inferior formability compared to B1.1 material, but rather that the reduced ability to stretch is noted and needs to be addressed for the stamping condition of interest (part design, die design, lubricant, etc.) and the higher lap-shear strength may be a benefit to reducing delamination. Clearly, the viscoelastic material can have a significant impact on the formability compared to the skin sheet material.

4. Summary and Conclusions

(1) The goal of this work was to understand the relationship between adhesion properties, tensile strength, and forming behavior of laminated steels. The adhesive properties, including the tensile lap-shear and 180° T-peel strengths, were determined for laminated steel constructed of three different viscoelastic cores in both 0.9-mm and 1.1-mm gages. For all the materials tested, little difference was found between properties in the longitudinal and transverse directions.

(2) The laminate delamination modes in T-peel tests were evaluated by optical and XPS analyses. Laminates in types A and C separated primarily by adhesive failure while type B laminate material exhibited thin-film cohesive failure.

(3) Examination of the test coupons suggests that the addition of inorganic conductive particles or powder may have only a small influence on the adhesive strength of laminated steel products because of the small geometric area that they affect. However, if the particles form large heterogeneous agglomerates that prevent adhesion over a significant area, the adhesive strength should decrease.

(4) Material tensile data is consistent among the laminated steels. The skin sheets have much greater mechanical properties than the relatively weak and thin viscoelastic core, and thus, dominate tensile behavior.

(5) Forming limit diagrams, which show the relative formability of the laminated steel materials, indicate that laminate formability was limited by the properties of the skin sheet material. In general, the formability of the

1.1-mm thick laminate was found to be less than that of the much thinner 0.55-mm thick skin sheet material and would be much less than that of a solid 1.1-mm thick sheet.

(6) The forming limit diagrams also indicate that the viscoelastic core material affects formability of laminated steel. For example, type A's formability is reduced in the plane strain region compared to the skin sheet whereas type B's formability is somewhat reduced in the draw region due to the presence of the viscoelastic core.

Acknowledgments

The authors wish to thank Jessica Schroeder and John Carsley for valuable discussion of the results, Maria Militello and Stephen Gaarenstroom for their XPS analysis of the laminated steel samples, Terrence Wathen for the training and assistance on the Instron equipment. John Carsley and Xiaohong Gayden are acknowledged for their helpful comments editing this report.

References

1. M.D. Rao, Recent Applications of Viscoelastic Damping for Noise Control in Automobiles and Commercial Airplanes, *J. Sound Vib.*, 2003, **262**(3), p 457–474
2. T. Saito and N. Mizuhashi, Resistance Welding of Vibration-Damped Steel Sheet, *Weld. Int.*, 1990, **4**(12), p 993–997
3. H. Oberle, C. Commaret, R. Magnaud, C. Minier, and G. Pradere, Optimizing Resistance Spot Welding Parameters for Vibration Damping Steel Sheets, *Weld. J.: Weld. Res. Suppl.*, January, 1998, p 8s–13s
4. S. Dinda, K.F. James, S.P. Keeler, and P.A. Stine, *How to Use Circle Grid Analysis for Die Tryout.* ASM International, 1981, p 3-7–3-9
5. J.K. Kim and P.F. Thomson, Forming Behavior of Sheet Steel Laminate, *J. Mater. Process. Technol.*, 1990, **22**(1), p 57
6. J.K. Kim and P.F. Thomson, Forming Behaviour of Sheet Steel Laminate, *J. Mater. Process. Technol.*, 1990, **22**(1), p 50
7. J.K. Kim and T.X. Yu, Forming and Failure Behaviour of Coated, Laminated and Sandwiched Sheet Metals: A Review, *J. Mater. Process. Technol.*, 1997, **63**, p 37